The Continuous Countercurrent Moving-Bed Separator

An investigation of the continuous chromatographic separation of an equimolar mixture of 1,3,5-trimethylcyclohexane and 1,3,5-trimethylbenzene with a 2.4 m × 1.37 cm ID vertical countercurrent moving bed is reported. The solid adsorbent was 30 mesh Al_2O_3, and the separation was carried out at 200°C. Steady-state axial concentration profiles of each species were determined by withdrawing vapor samples for analysis by gas chromatography. The binary mixture was continuously fed through a port located at approximately the midpoint of the column. The relative solids and carrier gas flow rates could be adjusted so that the more strongly adsorbed trimethylbenzene was transported downward, and less strongly adsorbed trimethylcyclohexane moved upward. For low feed rates, high-purity product streams of each were obtained at the bottom and top of the separator. For sufficiently high feed rates, trimethylbenzene was transported upward as well as downward, and top product purity deteriorated. This behavior is in qualitative accord with the predictions of a dispersionless, one-dimensional flow, adsorption equilibrium model incorporating a Langmuir isotherm.

Barry B. Fish
Robert W. Carr
R. Aris
Department of Chemical Engineering and Materials Science
University of Minnesota
Minneapolis, MN 55455

Introduction

Continuous separation of a binary mixture into two high-purity product streams, or of multicomponent mixtures into two fractions, may be accomplished with a countercurrent moving-bed separator (CMBS). Separation occurs during countercurrent contact of a flowing bed of granular material with a stream containing the separable mixture in an inert carrier fluid. Mixtures are separable provided the components have differing affinities for the solid. The relative solid-fluid flow rates are adjusted so that the component(s) interacting more strongly with the solids is carried along with them, while the component(s) interacting more weakly moves with the fluid phase. Also, the solid may be coated with a liquid that is usually called the stationary phase in conventional column gas-liquid partition chromatography (GLPC). Thus the term separator, used here, may be preferable to the more conventional "adsorber," since the latter implies separation by adsorption on a solid adsorbent, while the former is more general in that separation by GLPC is not excluded. In this sense, the countercurrent separation may be viewed as a continuous chromatographic process.

Falling-bed adsorption columns have been known for more than forty years. Berg (1946) described the hypersorption process in which activated carbon, flowing continuously downward in a vertical column, separates ethylene from a rising stream of hydrocarbon gases. With the advent of gas-liquid partition chromatography (James and Martin, 1952), falling-bed adsorption could be readily seen to be a continuous chromatographic process, although workers thirty years ago were more enamored of the analogy with extractive distillation. By the early 1960's several successful laboratory demonstrations of difficult binary separations had been reported in countercurrent moving beds (Scott, 1958; Pichler and Schulz, 1958; Barker and Critcher, 1960; Fitch et al., 1962; Schultz, 1963). Also, efficient separation of tertiary mixtures by using a falling-bed apparatus consisting of a major column and a side arm was demonstrated (Barker and Huntington, 1966). Barker (1971) reviewed the early experimental work, discussed simple criteria for separation, and showed axial concentration profiles, obtained during steady state operation of a CMBS, illustrating the applicability of these criteria.

Several mathematical models have been developed for the CMBS. Kasten and Amundson (1952) modeled an isothermal CMBS having one-dimensional flow of porous, spherical particles, one-dimensional fluid flow, and a single-component fluid

Correspondence concerning this paper should be addressed to R. W. Carr.
The present address of B. B Fish is Union Carbide Corporation, South Charleston, WV.

phase entering at the bottom of the column. For fluid-solid equilibrium and a linear isotherm, an analytical solution was obtained. Concentration profiles of the single adsorbate were given. An equilibrium one-dimensional flow model differing from Kasten and Amundson in that the feed is introduced at a side port, and external mass transfer to the solid particles is rate controlling, also yields analytical solutions (Yoon and Kunii, 1971). Model simulations of single-component concentration distributions are in excellent agreement with experimental data. Mass transfer coefficients were obtained in the region of low Reynolds number. Sherwood numbers were reported to be comparable to those for fixed and fluidized beds. A comprehensive equilibrium theory of multicomponent countercurrent exchange, including transient behavior, has also been developed (Rhee et al., 1970 a, b). Boundary discontinuities and, with a Langmuir isotherm, concentration shock waves arise from the dispersionless model. Asymptotic solutions to CMBS equations with axial dispersion and interphase mass transfer were published in a subsequent paper (Rhee and Amundson, 1973). Applications were illustrated by using the Langmuir isotherm. A recent review of continuous countercurrent systems included a model for adsorption of a single species obeying a linear isotherm and with axially dispersed flow (Ruthven, 1984).

Much of the theoretical work on the CMBS has employed linear isotherms, and many experiments have been done with dilute fluid phases where the isotherm is approximately linear. It has been shown that for a linear isotherm a simple criterion for a binary separation is given by $k_A < U_g/U_s < k_B$, where k_A and k_B are the partition coefficients of species A and B, respectively, and U_g and U_s are the fluid and solid flow rates (Barker and Critcher, 1960). With this criterion satisfied, A moves with the fluid phase and B moves with the solid. For production work, however, high throughput is desirable and operation in the nonlinear region of the isotherm may be necessary. Since the solids have finite capacity for adsorbate, at high feed rates the solids become saturated, and the more strongly adsorbed species, which would be carried downward with the solids at low concentration, travels upward in the column, and product purity deteriorates. The term flooding is used here to describe this situation.

This paper examines the countercurrent moving-bed separator under conditions in which a linear isotherm is not applicable. A mathematical model incorporating a Langmuir isotherm is developed, and the method of characteristics is employed to investigate the behavior of the CMBS. The results of an experimental investigation are also presented. Experimentally determined axial concentration profiles confirm model predictions. Conditions for attaining high product purity when the isotherm is nonlinear are found.

Theory: Countercurrent Separator

A countercurrent separator model is analyzed with a view to gaining physical insight into separator behavior, and to provide a framework for understanding the results of the experimental investigation. The Langmuir isotherm is used in all cases. We first consider a model for a single component, and apply the method of characteristics to the transient problem for a range of initial concentrations. Since the experimental investigation is of a gas-solid system, the theoretical development uses gas-solid nomenclature and language, although in principle it is applicable to liquid-solid systems as well.

The model asssumes one-dimensional flow of solids and gas, adsorption-desorption equilibrium, and neglects axial dispersion. This is termed the ideal model. Although finite mass transfer and dispersion are important when trying to size a separator, for our purpose these factors tend to complicate the physical interpretation and therefore will be neglected in this development.

The overall transient mass balance on the isothermal separator cross section is given by Eq. 1.

$$\epsilon \frac{\partial C}{\partial t} + (1 - \epsilon) \frac{\partial n}{\partial t} + \epsilon U_g \frac{\partial C}{\partial x} - (1 - \epsilon) U_s \frac{\partial n}{\partial x} = 0 \qquad (1)$$

Since the behavior for a linear isotherm provides a convenient point of departure for understanding operation under the influence of a nonlinear isotherm, a brief digression on the linear isotherm is presented here. When adsorption is fast, and the isotherm is linear, n can be realted to C at any point inside the column by the isotherm:

$$\frac{n}{N} = KC \qquad (2)$$

The transient mass balance reduces to

$$(1 + k) \frac{\partial C}{\partial t} + U_g (1 - \sigma) \frac{\partial C}{\partial x} = 0 \qquad (3)$$

where

$$k = \frac{1 - \epsilon}{\epsilon} NK$$

and

$$\sigma = \frac{1 - \epsilon}{\epsilon} \frac{U_s}{U_g} NK \qquad (4)$$

Equation 3 has the same form as its counterpart in pulsed column chromatography (Karger et al., 1973).

$$(1 + k) \frac{\partial C}{\partial t} + U_g \frac{\partial C}{\partial x} = 0$$

Since an adsorbable species moves at a velocity given by $V = U_g/(1 + k)$ in a fixed bed, then in the countercurrent moving bed the velocity is:

$$V = U_g \frac{1 - \sigma}{1 + k} \qquad (5)$$

For $\sigma > 1$, V is negative and a component moves downward in the column, while for $\sigma < 1$ a component moves upward. For $\sigma = 0$, corresponding to a fixed bed, Eq. 3 reduces to the above expression for pulsed column chromatography (Karger et al., 1973). To separate two components in a countercurrent moving bed, the operating conditions are adjusted so that $\sigma > 1$ for the more strongly adsorbed species, and $\sigma < 1$ for the less strongly adsorbed species. From Eqs. 4 and 5 it can be seen that for a linear adsorption isotherm, the velocity at which a species travels through a chromatographic medium is independent of its

concentration. The net molar flux of a component is given by Eq. 6.

$$f = \epsilon U_g C - (1 - \epsilon) U_s n \tag{6}$$

For a linear isotherm this becomes

$$f = \epsilon U_g C(1 - \sigma) \tag{7}$$

In this case the flux is directly proportional to the gas phase concentration for the given operating conditions.

These ideas are readily extended to the case of the Langmuir isotherm, which represents the fact that the solids have a finite carrying capacity. This isotherm is frequently found to give a more satisfactory description of adsorption than the linear isotherm.

$$\frac{n}{N} = \frac{KC}{1 + KC} \tag{8}$$

At low concentrations, $KC \ll 1$, and the isotherm becomes linear. Equation 8 can be substituted into Eq. 1 to give:

$$\frac{\partial \gamma}{\partial t}\left[1 + \frac{k}{(1 + \gamma)^2}\right] + \frac{\partial \gamma}{\partial x}\left[U_g - \frac{U_g \sigma}{(1 + \gamma)^2}\right] = 0 \tag{9}$$

where $\gamma = KC$.

The method of characteristics can be used to solve this transient problem. If $\gamma = \gamma[x(s), t(s)]$, then

$$\frac{d\gamma}{ds} = \frac{\partial \gamma}{\partial x}\frac{dx}{ds} + \frac{\partial \gamma}{\partial t}\frac{dt}{ds} \tag{10}$$

Let

$$\frac{dx}{ds} = U_g - \frac{U_g \sigma}{(1 + \gamma)^2}$$

and

$$\frac{dt}{ds} = 1 + \frac{k}{(1 + \gamma)^2} \tag{11}$$

Then

$$\frac{d\gamma}{ds} = 0 \tag{12}$$

and γ is constant along a line in the $[x(s), t(s)]$ plane described by $x(s), t(s)$.

$$\frac{dx}{dt} = \frac{U_g\left[1 - \frac{\sigma}{(1 + \gamma)^2}\right]}{1 + \frac{k}{(1 + \gamma)^2}} \tag{13}$$

For a given set of operating conditions, dx/dt is a function of only γ and dx/dt is the velocity of a point of concentration γ. From the initial conditions given, dx/dt locates a particular concentration as time proceeds. It is not the velocity of the species. If the mass transfer process between solid and gas phases is very fast, the velocity at which a component travels is:

$$V = (\text{fraction in gas phase})U_g - (\text{fraction adsorbed})U_s$$

$$V = \frac{\epsilon C U_g - (1 - \epsilon)U_s n}{\epsilon C + (1 - \epsilon)n} = \frac{U_g\left(1 - \frac{\sigma}{1 + \gamma}\right)}{1 + \frac{k}{1 + \gamma}} \tag{14}$$

Equation 14 is the analog of Eq. 5 for the case of a Langmuir isotherm. In this case, however, the velocity is concentration dependent, and for fixed σ, a species may have positive (upward) or negative (downward) velocity, depending upon whether $\sigma/(1 + \gamma) < 1$ or $\sigma/(1 + \gamma) > 1$, respectively. For a particular γ, we can calculate dx/dt and draw this slope in the (x, t) plane, starting with the initial value of γ at a particular position x at $t = 0$. These lines are the characteristic ground curves. If the characteristic ground curves cross, a concentration discontinuity must develop which satisfies the requirement that no mass or energy will accumulate at the shock. This criterion gives:

$$V_s = U_g \frac{\left[1 - \frac{k}{(1 + \gamma_1)(1 + \gamma_2)}\right]}{1 + \frac{k}{(1 + \gamma_1)(1 + \gamma_2)}} \tag{15}$$

where γ_1 and γ_2 are taken on opposite sides of the shock front. A complete treatment is given by Rhee et al. (1986).

The influence of a nonlinear isotherm on the behavior of the countercurrent side-fed separator can be introduced by first considering a configuration with no side feed, and $\sigma > 1$. In this situation, represented in Figure 1, a single species is present in the column, and its concentration is constant indefinitely above position $x°$ at $t = 0$ so that end effects can be neglected. Below $x°$, the concentration is zero everywhere. This example investigates the relation between the species flux and velocity, and the effect of the Langmuir isotherm as $C°$ is increased from very dilute to high concentration.

When $C°$ is very small, making $\gamma \ll 1$, Eq. 13 reduces to

$$dx/dt = U_g(1 - \sigma)/(1 + k) \tag{16}$$

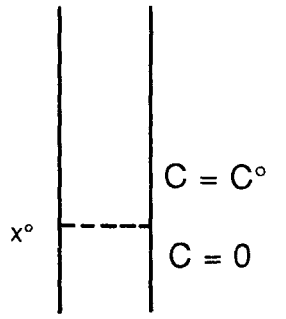

Figure 1. CMBS with a single species having $C = C°$ everywhere above $x°$, and $C = 0$ everywhere below $x°$, at $t = 0$.

the characteristic curves are not functions of γ, and Eq. 16 is equivalent to the result obtained for a linear isotherm. In this case, dx/dt is the velocity at which a species travels, since the flux is proportional to the gas phase concentration. If the initial concentration profile is given by Figure 2a, the front moves down the column at a velocity given by Eq. 16.

Now let C° be small, but large enough that γ is not negligible with respect to 1 and small enough that $dx/dt < 0$. The initial concentration profile is given in Figure 2b. At x° the concentration is C°. At some very small distance below x°, $x^\circ - \Delta x$, the concentration falls to zero. Between x° and $x^\circ - \Delta x$, all values of concentration between zero and C° exist. The slopes of the characteristic ground curves for $0 < C < C^\circ$ can be found using Eq. 13, and are sketched in Figure 2b. At x° the characteristics fan out due to the existence of all concentration values less than C°. The characteristics do not cross at x°. At some later time, t_1, the concentration profile can be found from Figure 2b by drawing a horizontal line at t_1. The concentration at any point (x, t_1) can be found by following the characteristic through (x, t_1) back to the $t = 0$ axis, along which the initial concentration profile was specified. A profile at an arbitrary t_1 is given in Figure 2c. The area of constant concentration has moved below x°, and the slope of the curve between C° and $C = 0$ has changed.

When C° is large enough to give dx/dt a positive slope, the characteristic ground curves will be given Figure 3a, and the concentration profile at t_1 by Figure 3b. At x° there is a vertical characteristic, which indicates that the concentration at this point will not change with time, no matter how large C° becomes. The vertical characteristic, $dx/dt = 0$, occurs when $\gamma = \sqrt{\sigma} - 1$. This concentration is denoted by γ^*.

It is now worthwhile to examine these results in terms of the flux. The net flux is given by Eq. 17, from which it is seen that the flux is concentration dependent.

$$f = \epsilon C U_g - (1 - \epsilon)\, n U_s = \epsilon C U_g \left(1 - \frac{\sigma}{1 + \gamma}\right) \qquad (17)$$

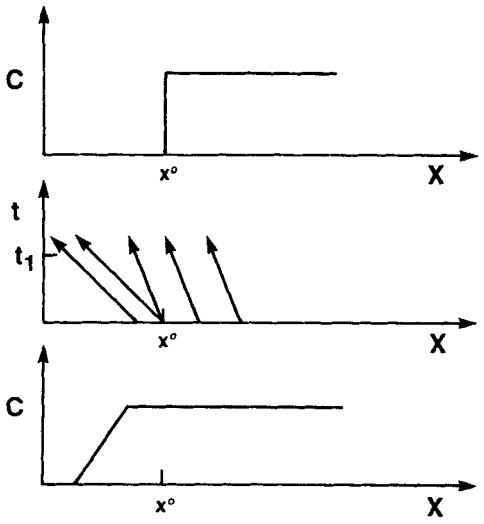

Figure 2. a. Axial concentration profile corresponding to Figure 1.
b. Characteristic ground curves, by Eq. 13, for the situation of Figure 2a and C° small.
c. Concentration profile at $t_1 > 0$.

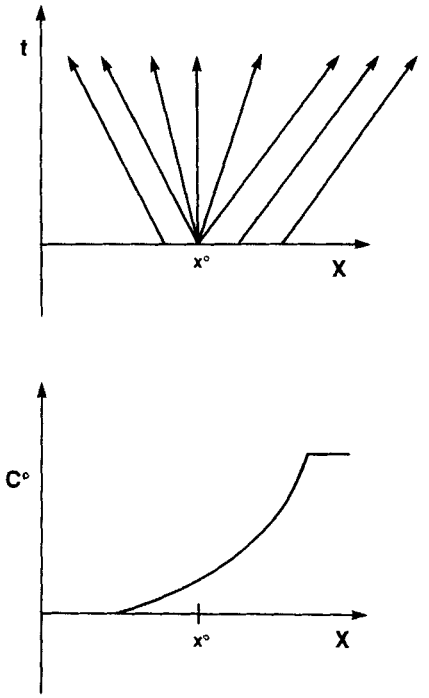

Figure 3. a. Characteristic ground curves, by Eq. 13, for the situation of Figure 2a and C° large.
b. Concentration profile at an arbitrary time $t > 0$.

For $\sigma > 1$, Figure 4 shows f vs. γ. At low concentration, the flux is negative; that is, there is a downward flux. As the concentration is increased, the downward flux initially becomes greater, then lessens, passes through zero, and becomes positive, at which point the net flux has turned about and is now upward in the column. The maximum downward flux occurs at $\gamma^* = \sqrt{\sigma} - 1$, and the flux passes through zero at $\gamma = \sigma - 1$. Note that the concentration at maximum downward flux corresponds with the vertical characteristic. Values of γ between $\sqrt{\sigma} - 1$ and $\sigma - 1$ give characteristic curves with positive slopes, even though the flux is downward everywhere in the column. This can be under-

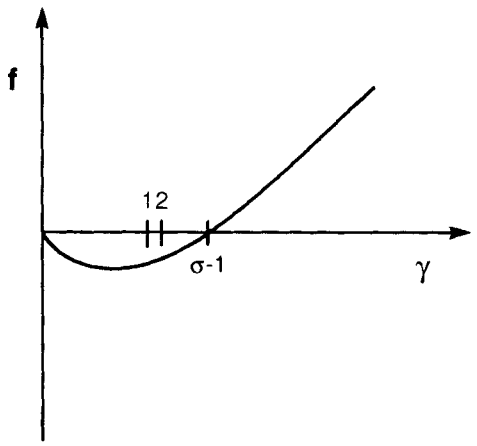

Figure 4. Net flux of a species with $\sigma > 1$ as a function of dimensionless concentration γ.
Positions 1 and 2 correspond with Figure 5

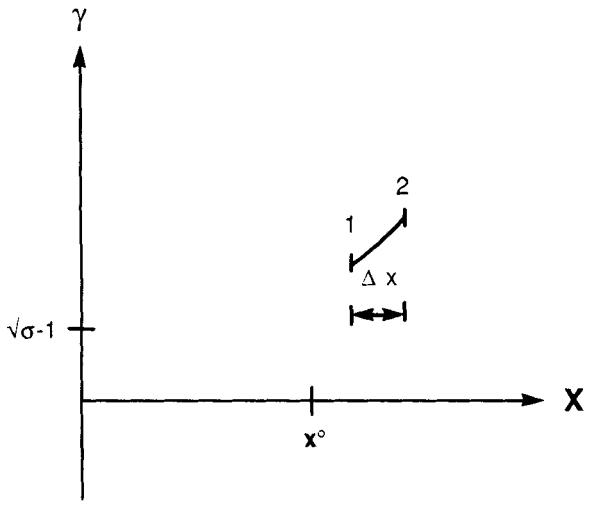

Figure 5. Concentration profile just above $x°$ at a time shortly after $t = 0$, for dimensionless concentrations between $\sqrt{\sigma} - 1$ and $\sigma - 1$.

stood as follows. Figure 5 is a diagram of the concentration profile just to the right of $x°$ immediately after $t = 0$. At position *1* in Figure 5 the downward flux is larger than the downward flux at position *2*. Therefore, the concentration between these positions begins to drop. This lower concentration value had previously been located to the left of its present position, and now has moved to the right, indicated by a positive dx/dt, even though the actual flux is downward. For $\gamma° > \sigma - 1$, the flux is upward

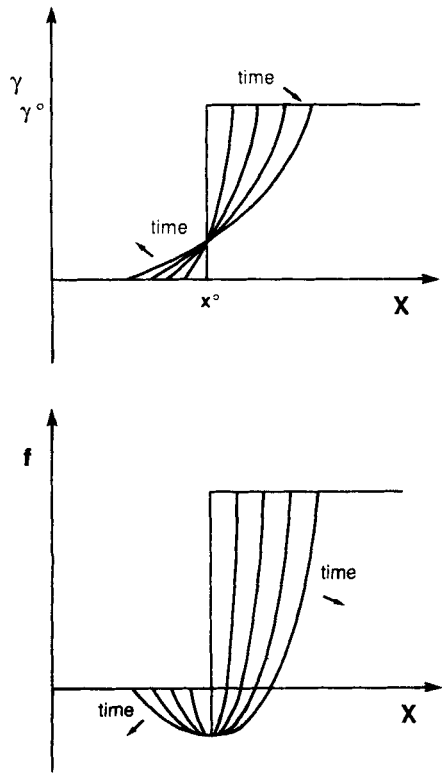

Figure 6. a. Concentration profiles as time proceeds. b. Net flux profiles as time proceeds.

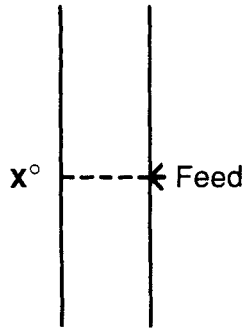

Figure 7. CMBS with side-feed configuration.

to the right of x_0, but is still the maximum downward value at $x°$. The concentration profile and flux profile are given in Figure 6.

The case $\sigma < 1$ is less interesting since the velocity and the flux are always upward.

Now consider the side-fed configuration, shown in Figure 7, for the case $\sigma > 1$. We would like to know the concentration profile inside the column for any feed rate F. Let F have units of moles · (time)$^{-1}$ · (cross-sectional areas of column)$^{-1}$. At low enough feed rate that $\sigma/(1 + \gamma) > 1$, the flux is downward, and the gas phase concentration below the feed can be found from Eq. 17. The maximum downward flux is $f_{max} = (-\epsilon U_g/K)(\sqrt{\sigma} - 1)^2$, and the corresponding concentration is $\gamma = \sqrt{\sigma} - 1$. This concentration corresponds to the vertical characteristic. The concentration at the position of origin of the vertical characteristic is constant, independent of the concentration above the position. Therefore, for feed rates producing fluxes less than or equal to f_{max}, all of the feed moves downward. If the feed rate is larger than this, since the species fed can only move downward at f_{max}, a portion of the feed has no choice but to move upward. To move upward, the concentration must be greater than $\sigma - 1$; see Figure 4. For these higher feed rates, a concentration discontinuity must develop at the feed point. The section of adsorber below the feed will be unaffected by larger feed rates, Figure 8. This behavior is a manifestation of the finite carrying capacity of the solid, due here to the use of the Langmuir isotherm.

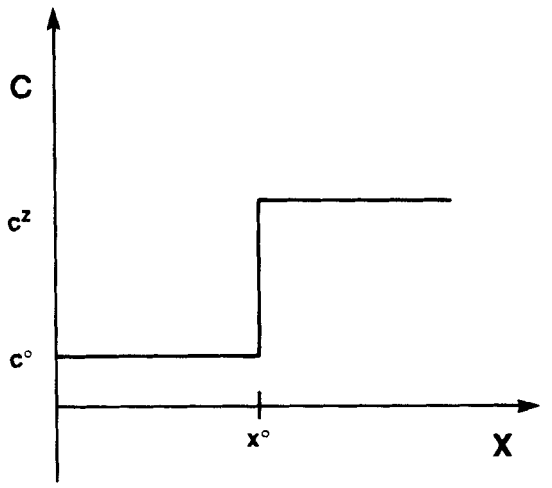

Figure 8. Steady-state concentration profile for side-feed configuration, $\sigma > 1$, and $C°$ large.

Boundaries of the separator

Consider the following steady-state situation with one component moving through the CMBS, and $\sigma < 1$, or if $\sigma > 1$, then $\gamma > \sigma - 1$, so the adsorber is being flooded. A mass balance on a section above the feed port and the top, Figure 9, gives Eq. 18.

$$n^t(1-\epsilon)U_s - U_g\epsilon C^t = n(1-\epsilon)U_s - U_g\epsilon C \qquad (18)$$

or $\nu^t\sigma - \gamma^t = \nu\sigma - \gamma$ after rearrangement. At a distance far from the top of the adsorber, γ and ν can be assumed to be related by the isotherm $\nu = \gamma/1 + \gamma$. For fresh, clean solids entering the top, $\nu^t = 0$, and

$$\gamma^t = \gamma - \frac{\gamma}{1+\gamma}\sigma \qquad (19)$$

If mass transfer is infinitely fast, then the clean solids entering immediately come to adsorption equilibrium just inside the top of the separator, and Eq. 20 is the balance at the top, where γ^{t-} is the gas phase concentration just inside the top.

$$\gamma^t = \gamma^{t-}\left(1 - \frac{\sigma}{1+\gamma^{t-}}\right) \qquad (20)$$

The ideal model thus predicts a concentration discontinuity at the separator outlet. A similar analysis at the bottom shows that a concentration discontinuity may occur there also. The effect of dispersion, and also mass transfer if it is not rapid enough, would be to cause the concentration profile to change over finite distance near each end.

A sharp concentration gradient at the top of the CMBS is not desirable, since the product concentration taken from a position immediately above the top is less than the concentration just inside the top. An improvement can be made by a slight change of configuration, Figure 10. If a portion of the gas phase is taken as the product stream from a point below the top, the concentration difference between the product stream and the gas inside the separator can be decreased, and ideally eliminated. A large enough fraction of the gas flow is taken at this point that the velocity above is reduced, making $\sigma_u > 1$. Thus the movement of adsorbate will be downward, and all of the adsorbate will exit with the product stream, which is enriched in adsorbate, while

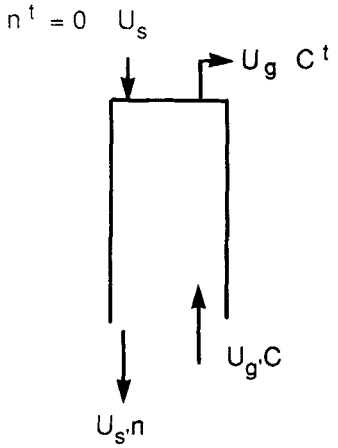

Figure 9. Normal top boundary condition.

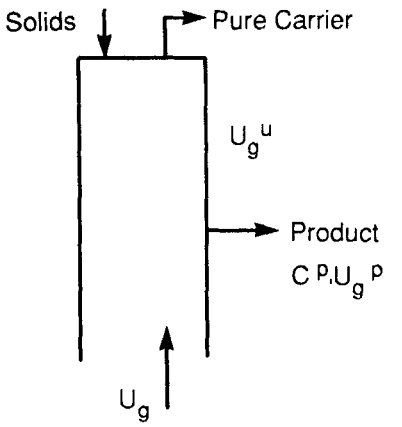

Figure 10. Modified top take-off configuration.

the carrier exiting the top is free of adsorbate, and may be recycled.

$$\sigma_u = \frac{1-\epsilon}{\epsilon}\frac{U_s NK}{(U_g - U_g^P)} \qquad (21)$$

A mass balance gives:

$$C^P\epsilon U_g^P = -n(1-\epsilon)U_s + U_g\epsilon C$$

or

$$\frac{C^P}{C} = \frac{U_g}{U_g^P}\left(1 - \frac{\sigma}{1+\gamma}\right) \qquad (22)$$

Equation 21 assumes that none of the adsorbate travels upward through the top section of the separator. Equation 22 shows that $C^P = C$ when

$$U_g^P = U_g\left(1 - \frac{\sigma}{1+\gamma}\right)$$

For these conditions, there is no concentration difference between the product stream and the top of the CMBS. But also at these conditions, $\sigma_u = 1 + \gamma$, by Eq. 21. This is exactly the point where σ_u has been decreased enough and γ^P has been increased enough such that the adsorbate is on the verge of moving upward through the top section of the adsorber. Therefore, the minimum product take-off stream allowed to collect all the species at the take-off port is:

$$\frac{U_g^{P_{min}}}{U_g} = \left(1 - \frac{\sigma}{1+\gamma}\right) \qquad (24)$$

If the product stream is smaller than $U_g^{P_{min}}$, the product concentration will remain equal to the column concentration, but some of the component will travel through the upper section, and leave the adsorber at the top, Figure 11. For $U_g^P > U_g^{P_{min}}$, all the product can be collected at the product take-off port, but there will be a concentration difference between the product concentration, and the concentration just inside the adsorber below the take-off port.

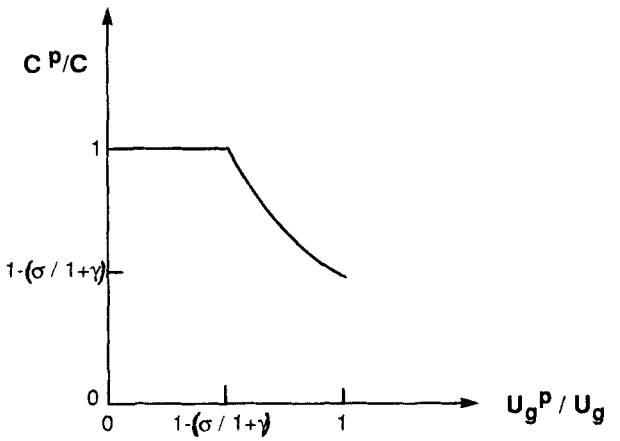

Figure 11. Output concentration vs. product flow rate.

Experimental System

Mixtures of trimethylcyclohexane (TMC) and mesitylene (MES) vapor were separated in a 2.4 m × 1.3 cm ID vertical stainless steel column, using 30 mesh Al_2O_3 adsorbent washed with a solution of KOH in methanol. The alcoholic KOH treatment apparently deactivates highly active surface sites, and produces a more nearly homogeneous surface with respect to adsorption, particularly for MES. Without deactivation some MES is so strongly adsorbed that stripping it from the Al_2O_3 is very difficult, and a significant amount of MES is invariably returned to the top with the solids recycle.

A diagram of the CMBS is given in Figure 12. Since a description of the computer-controlled apparatus has already been given (Fish et al., 1986), only a brief description is repeated here. Two recent modifications, a stripping section and a device to facilitate solids flow through the bottom orifice, are also described. The Al_2O_3 flows downward, while N_2 carrier gas is

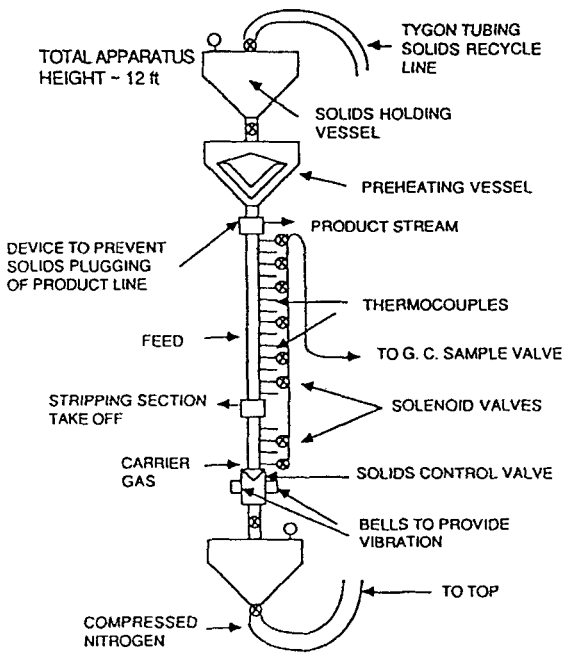

Figure 12. Countercurrent moving-bed separator.

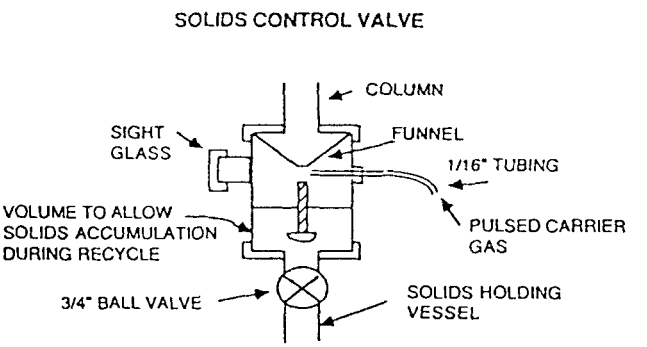

Figure 13. Solids flow regulation.

introduced at the bottom and travels upward. The feed enters at a position that may be chosen from several inlets located at intervals along the column. A syringe pump delivers the liquid feed, which vaporizes upon entering the column at its 200°C operating temperature. The solids are preheated and enter the column at the operating temperature. The solids flow rate is controlled by the valve shown in Figure 13. For these experiments, the required solids velocity put the gas flow near its upper limit (fluidization). Two electric bells are attached to the solids flow control valve to provide vibration, ensuring that the solids do not plug the orifice, and giving a constant flow rate. At very low flows, however, solid frequently clogs the orifice. To circumvent this difficulty, a 1.6 mm tube aimed just above the pin, Figure 13, conducts a short pulse of carrier gas at timed intervals to dislodge stationary solids. The pulse rate is approximately 0.6 s^{-1}. Each carrier gas pulse is accompanied by a vibration pulse from the bells. For each pulse, the solids travel roughly 2 mm in the column. This arrangement adds a pulsed mode to the carrier gas as well as to the solids, but the volume of the bottom vessel and solids flow valve acts as a capacitive filter, and tends to damp out the pulsed effect on the carrier gas.

The solids are collected in a vessel below the solids control valve. They are then recycled to the top by a N_2 gas lift. Valving allows isolation of the column during solids recycle so that continuous operation of the reactor may be maintained. The solids must be recycled about every 1.5 h. A run may last for 8 h.

To maintain high product purity, the solids must be free of any adsorbed species when they are recycled. The bottom 0.46 m of the column is used as a continuous on-line stripper. The carrier gas flow rate is higher in this section than in the section above it. There is an exit approximately 0.46 m from the bottom where a portion of the carrier is taken off, while the rest moves up the column. The flow rate in the stripping section is high enough so that $\sigma < 1$ for MES, and it ideally cannot travel downward through this section. This modification does not affect the ideal analysis, but will complicate the real comparison of experiment to theory due to the nonidealities around the bottom take-off port. The take-off stream may contain MES.

Results

In the first moving-bed experiments, only MES was fed. The operating parameters were adjusted so that $\sigma > 1$, and the MES was expected to move downward in the column at low feed rates. From the ideal model, a concentration jump is predicted to develop around the feed point as the feed rate is increased. Experimental data are shown in Figure 14. At low feed rates, all

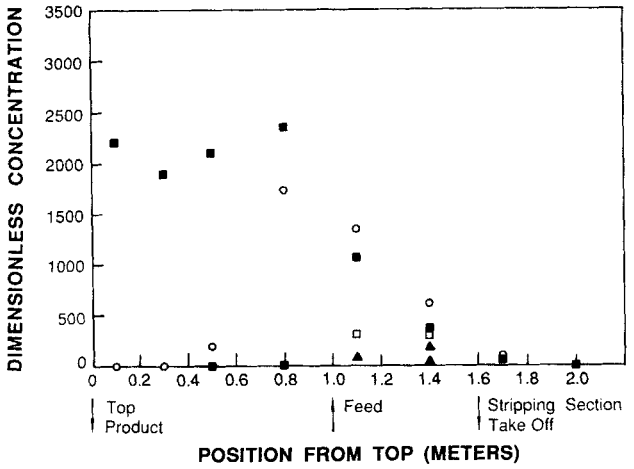

Figure 14. Mesitylene axial concentration profiles.

T = 200°C; Q = 1.3 L/min; U_s = 7.1 ±0.5 cm/min
Liquid feed rates: ▲ 0.154 mL/h; □ 0.271 mL/h; ○ 0.384 mL/h; ■ 0.575 mL/h.

the MES is seen to move downward. As the feed rate is increased, the concentration in the lower part of the separator increases, while the concentration above the feed port remains zero. At a feed rate of ≃ 0.384 mL/h, MES is present above the feed port, signaling the onset of flooding. At the next higher sample port, however, MES is still at a relatively low concentration. A steep concentration gradient exists in this region, and very little MES is transported to the top of the column. For a slightly higher feed rate, the concentration front moves upward and MES is eluted from the top. The position of the concentration front is an extremely sensitive function of feed rate in this operating range.

Figure 15 shows the concentration profile for TMC under the same solid and gas flow rates as were used in the MES experiments. For TMC, $\sigma < 1$ and the species velocity is expected to be upward for any feed rate. The experimental results confirm this. The concentration of TMC at the last sample port before leaving the adsorber is somewhat higher than the samples taken lower in the reactor. This is unexpected, and is probably due to nonuniform heating creating a locally high temperature and causing more TMC to desorb from the solids.

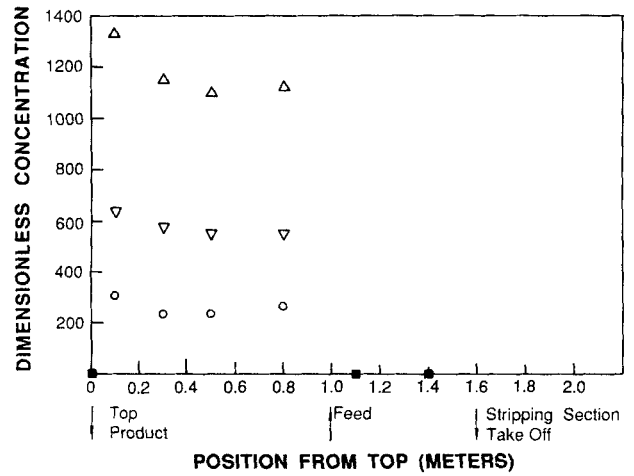

Figure 15. TMC axial concentration profiles.

T = 200°C; Q = 1.5 L/min; U_s = 7.1 ±0.5 cm/min
Liquid feed rates: ○ 0.154 mL/h; ▽ 0.384 mL/h; △ 0.770 mL/h.

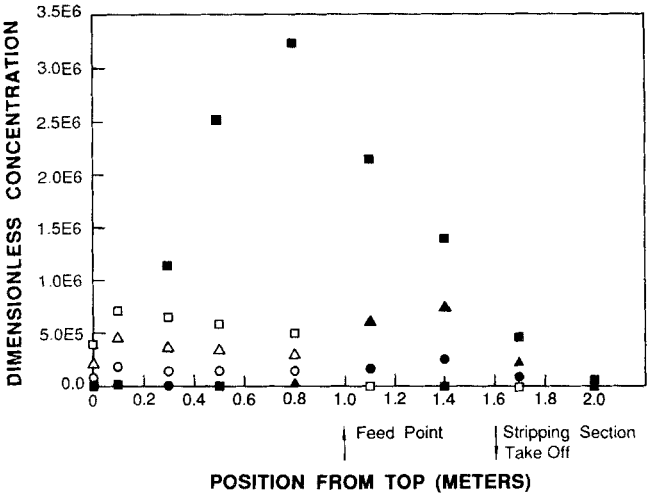

Figure 16. Axial MES and TMC concentration profiles, equimolar feed.

T = 200°C; Q = 1.5 L/min; U_s = 7.1 ±0.5 cm/min
Filled symbols, MES; open symbols, TMC
Total liquid feed rates: ○, ● 0.154 mL/m; △, ▲ 0.384 mL/h; □, ■ 0.770 mL/h.

Figure 16 shows the results when the CMBS was operated with a 50% TMC–50% MES (volume) mixture under the same operating conditions as the single-component runs. It is seen that the components are easily separable at low feed rates. At a feed rate of 0.77 mL/h the column is beginning to flood, and the CMBS is no longer capable of producing a pure product stream. For this feed rate, the data are not at steady state, and the MES front is moving slowly out of the adsorber. The product streams show the concentration difference between outside and 100 mm inside the adsorber. Figures 14 and 16 also illustrate the effectiveness of the stripping section in reducing the amount of MES leaving the bottom of the CMBS. Some of the MES still leaves, adsorbed on the alumina, and is recycled to the top. This is presumably the origin of the MES observed above the feed point when the column is not flooded.

Discussion

The experimental investigation shows that theoretical predictions of CMBS behavior are at least qualitatively borne out. However, there are some differences between predictions of the ideal model and experiment. The ideal CMBS model predicts that there is a maximum amount of MES that can be carried down the column. If the feed rate exceeds this downward transport rate, the carrying capacity of the solid is exceeded and flooding occurs. This produces a concentration discontinuity above the feed, and a concentration front that will move upward in the column. If the feed rate is just higher than the maximum downward flux, this concentration front will move upward at a very slow velocity. The experiments, however, show that nonidealities come into play. The concentration discontinuity at the feed does not exist, since some MES in excess of the maximum due to adsorption only presumably travels downward due to finite mass transfer. The upward edge of the concentration front moves slowly when the feed rate is just flooding the column, so that there is time for the leading edge to spread. The concentra-

tion front then gradually changes from a shock to a smooth curve. As the concentration decreases in the leading edge of the front due to uptake on fresh solid, the upward velocity decreases, and finally goes to zero. This situation leads to a fairly steep static concentration gradient in the upper part of the reactor.

In the ideal case, the concentration profile below the feed point should not change as the feed rate is increased. However, in the real case, the downward flux does increase somewhat, as can be seen in Fig. 14, where the gas phase concentration of MES increased below the feed point with increasing feed rate. This then must be due to dispersion and finite mass transfer caused by the concentration gradient around the feedpoint. Still, for feed rates large enough to flood the column, there is a large concentration difference between points just above and just below the feed. Feed rates high enough to cause flooding are not desirable if the adsorber is run as a continuous separator, but if this same configuration is used when a reversible reaction takes place on the solid surface, this may prove to be a useful region of operation.

Conclusions

An ideal mathematical model has been given which predicts the concentration profile around the feed point of a moving-bed separator as a function of feed rate. It was shown that for a species having $\sigma > 1$, there is a predicted maximum downward flux in the bed. Feed rates higher than this maximum result in flooding of the separator, and a concentration discontinuity around the feed point. This qualitative behavior has been observed in an experimental study. Flooding the column is undesirable, and the ideal model can be used to predict the maximum feed rate allowable for particular operating conditions if the more strongly adsorbed component follows the Langmuir isotherm. In fact, this maximum feed rate prediction is a lower bound on the true maximum allowable feed rate, because nonidealities in the real system allow for a larger downward flux in the column then predicted.

Acknowledgment

This work was supported by the Division of Chemical Sciences, Office of Basic Energy Sciences, U.S. Department of Energy, under Grant No. DOE-FG02-84ER13256.

Notation

C = gas phase concentration, mol/volume
f = net molar flux through any cross section, [=] mol/(time · area)
$k = (1 - \epsilon/\epsilon)\, NK$
K = adsorption equilibrium constant, 1/concentration
n = solid phase concentration, mol/volume
N = solid phase saturation concentration
Q = carrier gas flow rate
t = time
U_g = carrier gas velocity
U_s = solid phase velocity

Greek letters

$\gamma = K \cdot C$
$\gamma^* = \sqrt{\sigma} - 1$
ϵ = interparticle void fraction
$\nu = n/N$
$\sigma = (1 - \epsilon/\epsilon)\,(U_s/U_g)\, NK$

Superscripts

t = conditions outside top of adsorber
$t-$ = conditions just inside top of adsorber

Literature Cited

Barker, P. E., "Continuous Chromatographic Refining," *Prog. Separ. Purif.*, **4,** 325 (1971).
Barker, P. E., and D. Critcher, "The Separation of Volatile Liquid Mixtures by Continuous Gas-Liquid Chromatography," *Chem. Eng. Sci.*, **13,** 82 (1960).
Barker, P. E., and D. H. Huntington, *Advances in Gas Chromatography 1965,* A. Zlatkis and L. S. Ettre, eds. Preston Tech. Abstracts, Evanston, IL, 162 (1966).
Berg, C., "Hypersorption Process for Separation of Light Gases," *Trans. AIChE,* **42,** 665 (1946).
Fish, B., R. W. Carr, and R. Aris, "The Countercurrent Moving-Bed Chromatographic Reactor," *Chem. Eng. Sci.*, **41,** 661 (1986).
Fitch, G. R., M. E. Probert, and P. F. Tiley, "Preliminary Studies of Moving-Bed Chromatography," *J. Chem. Soc.*, 4875 (1962).
James, A. T., and A. J. P. Martin, "Gas-Liquid Partition Chromatography: The Separation and Microestimation of Volatile Fatty Acids from Formic Acid to Dodecanoic Acid," *Biochem. J.*, **50,** 679 (1952).
Karger, B. L., L. R. Snyder, and C. Horvath, *An Introduction to Separation Science,* Wiley, New York (1973).
Kasten, P. R., and N. R. Amundson, "Analytical Solution for Simple Systems in Moving-Bed Adsorbers," *Ind. Eng. Chem. Fundam.*, **44**(7), 1704 (1952).
Pichler, H., and H. Schulz, "Kontinuierliche Trennung von Gasen durch ein Neues Verfahren der Gegenstromverteilung," *Brennstoff-Chemie,* **39,** 148 (1958).
Rhee, H. K., and N. R. Amundson, "Asymptotic Solution to Moving-Bed Exchange Equations," *Chem. Eng. Sci.*, **28,** 55 (1973).
Rhee, H. K., R. Aris, and N. R. Amundson, *First-Order Partial Differential Equations,* **I,** Prentice Hall, Englewood Cliffs, NJ (1986).
———"Multicomponent Adsorption in Continuous Countercurrent Exchangers," *Phil. Trans. Roy. Soc. London A,* **267,** 187 (1970a).
———"On the Theory of Multicomponent Chromatography," *Phil. Trans. Roy. Soc. London A,* **267,** 419 (1970b).
Ruthven, D. M., *Principles of Adsorption and Adsorption Processes,* Wiley, New York (1984).
Schultz, H., *Gas Chromatography,* Van Swaay, ed., Butterworths, Lond, 225 (1963).
Scott, R. P. W., *Gas Chromatography,* Desty, ed., Butterworths, London, 287, (1958).
Yoon, S. M., and D. Kunii, "Physical Adsorption in a Moving Bed of Fine Adsorbents," *Ind. Eng. Chem.*, **10**(1), 64 (1971).

Manuscript received Aug. 26, 1988, and revision received Dec. 16, 1988.